Received: 30 November 2018 | Revised: 15 January 2019 | Accepted: 15 January 2019

DOI: 10.1002/mrc.4837

SPECIAL ISSUE RESEARCH ARTICLE

WILEY

Exploring the tumour extracellular matrix by in vivo Fast Field Cycling relaxometry after the administration of a Gadolinium-based MRI contrast agent

Simona Baroni[1] | Maria Rosaria Ruggiero[1] | Silvio Aime[1,2] | Simonetta Geninatti Crich[1]

[1]Department of Molecular Biotechnology and Health Sciences, University of Torino, Torino, Italy

[2]Istituto di Biostrutture e Bioimmagini (IBB), Consiglio Nazionale delle Ricerche, via Nizza 52, Torino, Italy

Correspondence
Prof. ssa Simonetta Geninatti Crich, Molecular Biotechnology and Health Sciences, University of Torino, via Nizza 52, Torino, Italy.
Email: simonetta.geninatti@unito.it

Funding information
European Cooperation in Science and Technology, Grant/Award Number: 15209; Horizon 2020 Framework Programme, Grant/Award Number: 668119; European Union's Horizon 2020 research and innovation programme, Grant/Award Number: 668119

Corrections added on 23 October 2019, after first online publication: Copyright line has been updated.

Abstract

^{1}H Fast Field Cycling NMR (FFC-NMR) relaxometry is proposed as a powerful method to investigate tumour stroma in vivo upon the administration of a Gd-based contrast agent. To perform this study, an FFC-NMR equipment endowed with a wide bore magnet was used for the acquisition of Nuclear Magnetic Resonance Dispersion profiles on healthy muscle and tumour tissue in living mice. At magnetic field strengths < of ca. 1 MHz, the differences in the relaxation rates of the intra and extracellular compartment become of the same order of magnitude of the exchange rate across the cellular membranes. Under this condition, the water exchange rate between the two compartments yields to a biexponential magnetization recovery that can be analysed by fitting the experimental data with the two-Site eXchange (2SX) model. Using this model, it was possible to obtain, for the two compartments, both relaxation properties and water kinetic constants for water exchange across cell membranes. The method allowed us to determine the effect of the "matrix" on the water proton relaxation times and, in turn, to get some insights of the composition of this compartment, till now, largely unknown.

KEYWORDS

Fast Field Cycling relaxometry, Gd contrast agents, intracellular water lifetime, tumour stroma

1 | INTRODUCTION

Magnetic Resonance Imaging (MRI) has got a key role in the field of oncology since few decades. Its prominent role relies on the superb spatial and temporal resolution of the images it can provide. The relaxation time T_1, a measure of how fast the nuclear spin magnetization returns to its equilibrium state after the application of a radiofrequency pulse, is a very important source of contrast in MRI. However, at the magnetic field strength of the currently available MRI scanners, changes in tissue T_1 do not appear sensitive enough to report on some peculiar aspects of the tumour.[1] The noninvasive differentiation between benign and malignant lesions (in breast cancer for example), relies on the use of Dynamic Contrast Enhancement MRI (DCE-MRI) protocols, based on the use of Gd-based contrast agents. This procedure provides important functional information related to the enhanced permeability of blood vessels in the tumour region. Diffusion-weighted imaging and MR spectroscopic imaging protocols have been implemented into the clinical practice to obtain additional functional parameters that may be simultaneously analysed in the so-called multiparametric imaging approach.[2] However, there is widespread opinion that, at low magnetic field strength, the marked increase of R_1 ($=1/T_1$) observed in biological tissues might be used

to improve the diagnostic potential of MRI in tumour phenotyping.[3–5] Although examples of $1/T_1$ Nuclear Magnetic Relaxation Dispersion (NMRD) profiles[6] acquired in the 0.01–20 MHz range on fresh or thawed surgical specimens were reported since the early 80s of the past century,[7] the interpretation of these data remains almost completely empirical due to the lack of suitable model theories for their correct and exhaustive analysis. Moreover, the use of ex vivo samples has the flaw that it cannot take into account the dynamics of water mobility, that is a key determinant of the NMRD profile. Fast Field Cycling (FFC) is the only practicable way of measuring T_1-dispersion; it involves switching the magnetic field between different field strengths, during the measurement procedure. Recently, the prognostic potential of the NMRD analysis has been highlighted by our group, using a prototype FFC relaxometer endowed with a wide bore magnet with a dedicated transmitter/receiver solenoid detection coil placed around the mouse's leg. Water proton $1/T_1$ NMRD measured in vivo on implanted mammary tumours showed a marked T_1 elongation at low magnetic fields (<0.2 T) with respect to healthy tissues.[8] The differences observed in the NMRD profiles allowed the discrimination between mammary tumours characterised by different metastatic potential such as 4 T1, TS/A, and 168FARN models. These differences are directly correlated to the exchange rate of water molecules across the membrane of the tumour cells. In fact, the observed T_1 is the result of the mixing between the relaxation rates of the intracellular (R_{1in}) and extracellular compartments (R_{1ex}), being V_{ex} and V_{in} the respective volume fractions (Figure 1). Differences in the relaxation rates of the two compartments are inversely proportional to the magnetic field strength, becoming of the same order of magnitude of the exchange rate across the cellular membranes at magnetic fields of ca. 0.025 T (i.e., at the Larmor frequency of ca. 1 MHz). Under this condition the water exchange rate between the two compartments yields to a biexponential magnetization recovery that can be analysed by fitting the experimental data with the two-Site eXchange (2SX) model.[9–14] Thus, the measurement at magnetic fields <1 MHz allow the exploration of water dynamics and the separation of the intracellular contribution from the one of the extracellular compartment. This is not possible at high magnetic fields because the similar values of the relaxation rates in the extra and intracellular compartments cause the occurrence of the fast exchange regime that makes the magnetization recovery mono-exponential with a relaxation rate that is an average between the values of the two compartments. Landis and coworkers[13] showed that, at the clinical imaging fields, the biexponentiality of the M_z-curve can be recovered if the extracellular relaxation rate R_{1ex} is "artificially" increased by the presence of paramagnetic contrast agents.

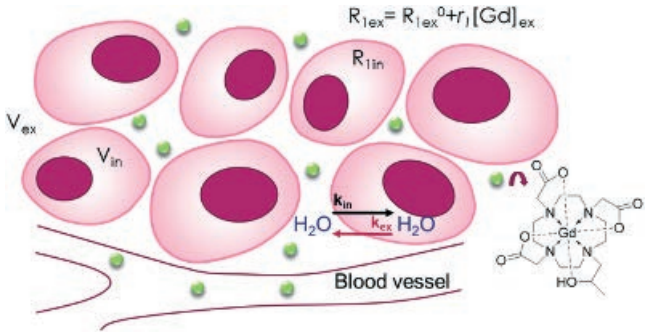

FIGURE 1 Schematic representation showing the extracellular distribution of ProHance (green circle) in the tissue. Water molecules reside inside the cells (V_{in} and R_{1in}) and in the extracellular space (V_{ex} and R_{1ex})

The aim of our work was to explore the role a paramagnetic contrast agent (CA), for example, Gd-HPDO3A (ProHance®, Bracco Imaging S.p.A., Milan, Italy), may have on the NMRD profiles acquired in vivo on murine models. On may expect that the paramagnetic agent may act as a reporter of the physicochemical characteristics of the "matrix" that defines the extracellular compartment (Figure 1). In the literature, some example of NMRD profiles acquired after the administration of paramagnetic agents on fresh surgical specimens,[15–17] are reported. However, the use of ex vivo samples has the drawback that it cannot take into account the dynamics of the CA distribution as well as the water mobility, that are the key determinants of the NMRD profile.

2 | MATERIALS AND METHODS

2.1 | Animal model

BALB/c mice (Envigo, Bresso, Italy) were maintained under specific pathogen free conditions in the animal facility of the Molecular Biotechnology Center, University of Turin and treated in accordance with the EU guidelines (EU2010/63).

Six-week-old female BALB/c mice were inoculated in their muscle hind limb with about 1 million of 4 T1 (Group 1, $n = 4$) or TS/A (Group 2, $n = 4$) tumour cells suspended in 100 μl of phosphate-buffered saline. A third group of untreated mice ($n = 6$) was used as control. Both cell lines were initially derived from a spontaneous breast tumour growing in a BALB/c mouse. 4 T1 (ATCC® CRL-2539™ purchased from American Type Culture Collection [ATCC, USA]) and TS/A (kindly provided by prof. F. Cavallo's group, University of Turin) were grown in RPMI 1640 medium supplemented with 10% fetal bovine serum, 100 U/ml Penicillin (P) with 100 μg/ml

Streptomycin (S) and 4 mM Glutamine (Gln). Cells were cultured in 5% CO_2/95% air at 37°C in a humidified chamber and were split every 2 to 3 days. All cells were tested negative for mycoplasma by MycoAlert™ Mycoplasma Detection Kit. All materials were purchased from Lonza (Basel, Switzerland).

Before undergo to NMR experiments, mice were anaesthetized with a mixture of tiletamine/zolazepam (Zoletil 100; Vibac, Milan, Italy) 20 mg/kg and xylazine (Rompun; Bayer, Milan, Italy) 5 mg/kg.

When tumours reached 10 mm mean diameter, mice were euthanized for ethical reasons.

2.2 | MRI

T_1-weighted images of the mouse limb region were acquired on a 7 T Bruker AV300 spectrometer equipped with a Micro 2.5 microimaging probe and a birdcage resonator with 30-mm inner diameter. The animals were anesthetised before MRI examination as described above. Images were recorded 1 day before the acquisition of the NMRD profiles, before and after the injection of ProHance (0.2 mmol/Kg). The distribution of ProHance in the tumour region was followed by measuring T_1 before and 7′, 13′, 20, 32′ after the contrast agent injection, by means of a saturation recovery sequence (TE = 3.3 ms; number of slices = 3; slice thickness = 2 mm; FOV 30 × 30 mm; matrix 32 × 32). The tumour volume was measured from T_2-weithed MRI images obtained by using a rapid acquisition with refocused echoes sequence protocol (TR = 5,000 ms; TE = 28 ms; number of slices = 11; slice thickness = 1 mm; FOV 50 × 50 mm; matrix 168 × 160).

Assuming the occurrence of a fast exchange regime (i.e.,$|R_{1in} - R_{1ex}| \ll k_{in} + k_{ex}$),[18] at 7 T, the effective intratumour ProHance concentration, $[Gd]_{eff}$, was determined by Equation 1

$$[Gd]_{eff} = (R_{1POST} - R_{1PRE})/r_1. \quad (1)$$

Where R_{1POST} and R_{1PRE} are the relaxation rates measured after and before the CA injection; r_1 is the millimolar relaxivity measured at 7 T of ProHance for a 1-mM solution in Matrigel ($r_1 = 4.86\ mM^{-1}\ s^{-1}$) used as extracellular matrix model. Matrigel is the trade name for a gelatinous protein mixture secreted by Engelbreth-Holm-Swarm mouse sarcoma cells produced and marketed by Corning Life Sciences and BD Biosciences.

The $[Gd]_{eff}$ is the effective value of the tissue concentration, as it refers to the sum of the intracellular and extracellular volumes. Then, the ProHance concentration in the extracellular volume fraction (V_{ex}) is given by Equation 2

$$[Gd]_{ex} = [Gd]_{eff}/V_{ex}. \quad (2)$$

2.3 | NMRD profile acquisition protocol

$1/T_1$ NMRD profiles of tumour bearing mouse (six points at 0.01, 0.025, 0.063, 0.158, 0.398, and 1 MHz) were acquired 10 days after cell inoculation on a Stelar SPINMASTER FFC NMR relaxometer (Stelar S.n.c., Mede [PV], Italy) equipped with a 40-mm 0.5-T FC magnet and a dedicated 11-mm solenoid detection coil. Data were acquired with a prepolarized sequence applied at 13 MHz and detection at 14.5 MHz, a field switching time of 4 ms, a 90° pulse length of 5.5 μs, and 32 incremented relaxation delay (logarithmic distributed from 0.01 to 2.8 s). The relaxometer operates under complete computer control with an absolute uncertainty in the $1/T_1$ value of ±2%.

The profiles were acquired pre and post the injection of 0.2 mmol/Kg dose of ProHance.

The magnetization recovery data were analysed according to a mono-exponential decay (Bloch equation) and the two-Site eXchange model (2SX model, see below) with Origin software (OriginPro 8.5.0 SR1, OriginLab, Northampton, MA, Levenberg–Marquardt algorithm).

3 | RESULTS AND DISCUSSION

The two-Site eXchange (2SX) model describes the time evolution of M_Z that depends on the absolute values of the relative size of the "relaxation" term, $|R_{1in} - R_{1ex}|$, and of the "exchange" term $k_{in} + k_{ex}$, (where $k_{in} = 1/\tau_{in}$ is the water exchange rate from the extracellular to the intracellular compartment and $k_{ex} = 1/\tau_{ex}$ is the water exchange rate in the opposite direction). This relationship was previously defined as the NMR "shutter-speed."[9,12,13] It is important to note that both R_{1in} and R_{1ex} depend on the magnetic field strength; their values are very similar at high magnetic field strength and progressively diverge on going to low magnetic field strengths, where $R_{1in} > R_{1ex}$.[8] R_{1ex} is influenced by the CA extravasation from blood capillaries to the extracellular space,[19] yielding $R_{1ex} = R_{1ex}^0 + r_1[Gd]_{ex}$, where R_{1ex}^0 is the contribution in the absence of exchange and CA and r_1 and $[Gd]_{ex}$ are the extracellular CA relaxivity and millimolar concentration, respectively. The values of the rate constants, k_{in} and k_{ex}, depend mainly on temperature, osmotic pressure, and cell metabolism.

In the range 0.01–1 MHz, that represents the proton Larmor frequencies at which the NMRD profiles were acquired, the predominant contribution arises from R_{1in}, and the condition $|R_{1in} - R_{1ex}| \sim k_{in} + k_{ex}$ is expected to be met, even in the presence of ProHance (that causes the increase of R_{1ex}). The system is in an intermediate-exchange regime, and the longitudinal ^1H_2O relaxation exhibits a biexponential experimental decay associated to two apparent contributions, one with the larger and one with the smaller longitudinal relaxation time. By the 2SX analysis of the M_z evolution, it is possible to dissect the two contributions and assess the ProHance r_1 value for the extracellular compartment. This method gives the possibility, for the first time, to explore the tumour extracellular matrix that regulates tumour cell migration and invasion, through the detection of the r_1. This parameter is a good reporter of the interactions the paramagnetic complex may have with the biomolecules of the microenvironment in which it distributes.

Thereafter, two mouse mammary adenocarcinoma cell lines, namely, TS/A and 4 T1, were injected in the muscle of the hind limb to obtain the corresponding tumour xenografts suitable for in vivo studies. In order to set-up the in vivo acquisition time interval of the NMRD profiles, ProHance was administered intravenously to mice bearing tumours with a volume that is >65% of the total leg + tumour tissue. The CA biodistribution dynamics were evaluated by measuring T_1 on a 7-T MRI scanner after the injection of ProHance at 0.2 mmol/kg dose. The experiment was carried out the day before the NMRD profile acquisition in order to deal with similar anatomical/functional conditions. The use of a high magnetic field strength ensured the occurrence of a fast exchange regime, that is, $|R_{1in} - R_{1ex}| \ll k_{in} + k_{ex}$, that makes the relaxation rate measurement independent on the presence of intra and extracellular compartments.

Figure 2 shows that the Gd concentrations ($[Gd]_{eff}$) found in both mammary tumour xenografts were significantly higher than those found in the healthy muscle. This is due to an increase of permeability of the neoformed vessels, often called enhanced permeation and retention, effect shown by many tumour types. By analysing the contrast dynamic behavior, the appropriate NMRD acquisition interval was set between 7 and 20 min after the ProHance injection (i.e., an acquisition time of 13 min, the grey area in Figure 2). During this time, the Gd complex concentration showed a variation of less than 30% in the tumour tissue (more precisely between 0.136 ± 0.018 mM and 0.123 ± 0.017 mM for 4 T1; between 0.140 ± 0.009 mM and 0.115 ± 0.006 mM for TS/A). The fast elimination of ProHance from the tumour tissue forced us to measure R_1 at a maximum of six magnetic field strengths, in the 0.01–1 MHz proton Larmor frequency range.

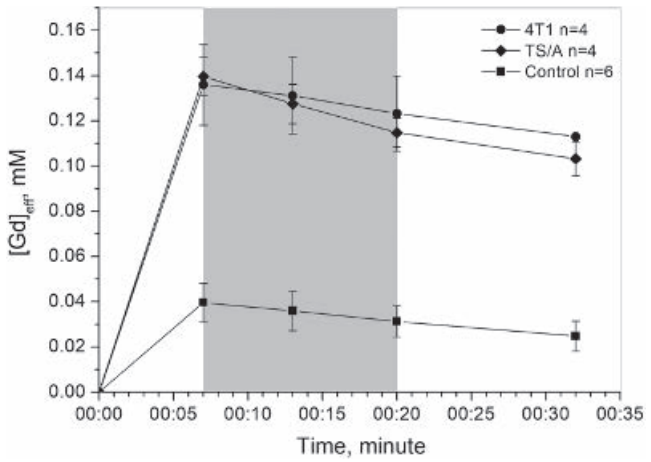

FIGURE 2 Estimated Gd-complex concentration in the 4 T1 (filled circle) and TS/a (filled diamond) tumour tissues and control legs (filled square) as a function of the time after i.V. administration. Concentration was estimated by T_1 measured at 7 T using Equation 1. The grey area indicates the time required for the Nuclear Magnetic Relaxation Dispersion profile acquisition

Figure 3 shows the observed relaxation rate R_1 values obtained by the monoexponential fitting of magnetization recovery for 4 T1 (on the left) and TS/A (on the right) tumours before and after the injection of ProHance. As expected, the relaxation rate measured after ProHance injection is higher than the PRE contrast value at any magnetic field strength. The enhancement of the relaxation rate (i.e., $[R_{1POST}\text{-}R_{1PRE}]/R_{1PRE}$) brought by ProHance markedly decreases as the applied magnetic field strength decreases. Basically, this is the consequence of the simultaneous increase of tissue relaxation rates (mainly due to the R_{1in} contribution as shown above) and the nearly constant ProHance relaxivity in this magnetic field range (Figure 4). A good model for the determination of T_1 in the presence of ProHance in the extracellular matrix is obtained by dissolving the CA in Matrigel, a gelatinous protein mixture secreted by Engelbreth–Holm–Swarm mouse sarcoma cells. It is a model of the extracellular environment found in many tissues and used as a substrate for cell cultures.[20]

Figure 4 shows the NMRD profile of ProHance dissolved in water and in Matrigel, and Table 1 reports the parameters obtained by the fitting for the inner- and outer-sphere contributions (Solomon-Bloembergen-Morgan and Hwang-Freed theory,[23,24] respectively). An increase of the rotational correlation time, τ_R, value of about 60% accounts for the different behavior, as a consequence of the higher viscosity of Matrigel. For both

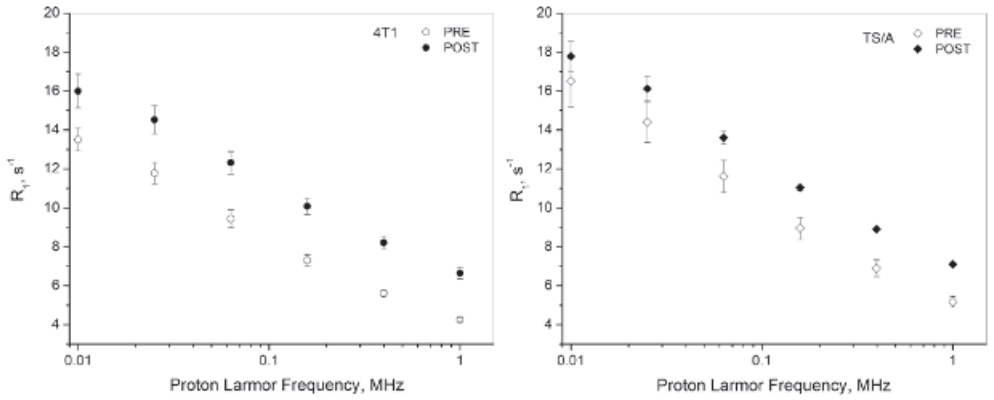

FIGURE 3 Nuclear Magnetic Relaxation Dispersion profile of tumour bearing (4 T1 on the left and TS/A on the right) mouse leg before (pre, open symbol) and after (post, filled symbol) the injection of ProHance. The number of animal tested was at least 4. Error bars report the standard deviation. During the saturation recovery acquisition, 32 tau values were spaced logarithmically from 7 m s to 2.8 s

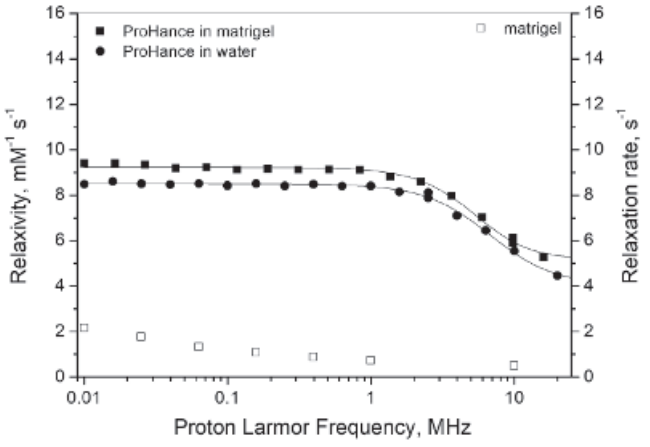

FIGURE 4 Nuclear Magnetic Relaxation Dispersion profile of ProHance in water (filled circle) and in Matrigel (filled square), referred to the left *y*-axis (25°C). The Matrigel contribution is also reported (open square), referred to the right *y*-axis

TABLE 1 Parameters obtained by the fitting procedure of the Nuclear Magnetic Relaxation Dispersion experimental data (25°C)

	Water	Matrigel
Δ^2 (10^{19} s^{-2})	4.6 ± 1	6.2 ± 0.6
τ_v (ps)	15 ± 2	15 ± 1
τ_R (ps)	53 ± 3	82 ± 3
τ_M (ns)	225[a,*]	
r (Å)	3.0*	
q	1*	
D (cm^2 s^{-1})	2.25e^{-5}*	2.0e^{-5}[b,*]
a (Å)	3.8*	

[a]The considered τ_M is the average value determined in water weighted over the relative isomeric population the ratio for the two possible coordination geometries SAP (capped square antiprismatic geometry) and TSAP (capped twisted square antiprismatic geometry) is 75% and 25%, respectively[21,22];

[b]the value was fixed taking into account the relative differences (14%) of the apparent diffusion coefficient measured by DWI-MRI (see supplementary material) in water and in Matrigel, respectively.

*Fixed during the fitting procedure.

profiles, the considered τ_M is the value determined in water. τ_M was not determined in Matrigel as this medium changes the physicochemical state from gel to liquid at $T < 22C°$. However, being τ_M determined by the enthalpy of the Gd-Ow bound, one can reasonably assume that it is not significantly affected on going from neat water to Matrigel.[25,26]

Next, the fitting of the magnetization recovery curves acquired as a function of the magnetic field strength on the two tumour models before the ProHance injection, was then performed according to the 2SX model taking into account the biexponential behavior of the magnetization. Data were simultaneously analysed, sharing the V_{ex} end τ_{in} parameters maintaining $R_{1ex}{}^0$ fixed to the Matrigel values obtained in a separated experiment (Figure 4). The V_{ex} was allowed to vary within a reasonable range, in accordance with results already reported in the literature (0.09–0.19 for healthy mouse hind limb, 0.15–0.5 for tumour mouse hind limb.[13,27–29] The R_{1in} admitted range was the one that previously reported on the same type of tumours.[8] The results obtained from the analysed NMRD profiles (six field values and 32 tau) on healthy mouse and tumour bearing one were comparable with those ones reported in our previous studies under slightly different conditions (10 field values and 48 tau, total time 32 min).[8] As expected, the tumour extracellular volume (V_{ex}) was higher than in healthy tissue, going from 0.13 ± 0.02 to 0.22 ± 0.01 and 0.26 ± 0.03 for healthy, TS/A, and 4 T1 tissues, respectively.[13,27–29] The opposite trend for the intracellular water residence time was confirmed (1.24 ± 0.1 s for healthy tissue, 1.12 ± 0.14 s for TS/A tumour model and 0.68 ± 0.16 s for the more aggressive 4 T1 tumour model).

In principle, the fitting of the NMRD data acquired after the ProHance injection involves a high number

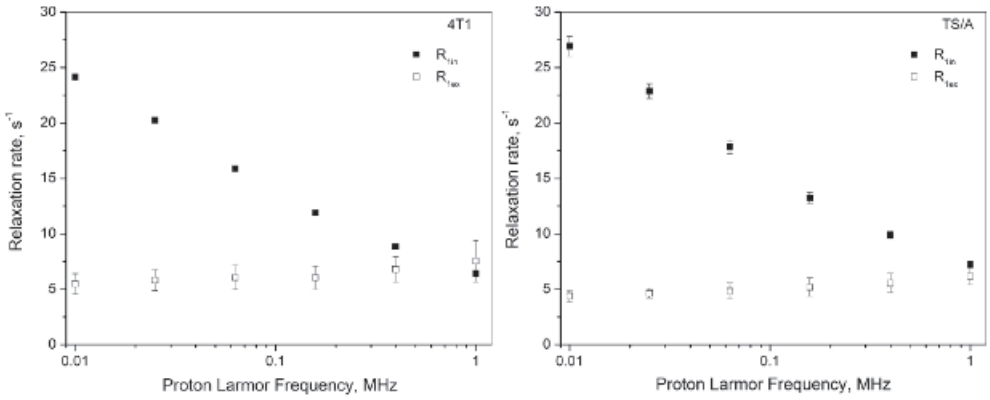

FIGURE 5 The relaxation rate contributions of the intracellular (filled square) and extracellular spaces (open square) obtained by analysing the M_z recovery curve acquired as a function of the magnetic field strength according to the 2SX model, as described in the text

($n = 6$) of unknown parameters (R_{1in}, R_{1ex}, τ_{in}, V_{ex}, $[Gd]_{ex}$, r_1 of the Gd-complex in the extracellular space of the tissue). Thus, for each mouse, the fitting was carried out by fixing: R_{1in}, V_{ex}, and τ_{in}, at the values found in the analysis of the corresponding PRE-contrast NMRD profiles. The $[Gd]_{ex}$ concentration value was the one from the contrasted images acquired at 7 T (Figure 2) assuming that the Gd-complex distribution is exclusively extra cellular (V_{ex}) and taking into account, the [Gd] decrease in the time interval (see Equations 1 and 2). The resulting R_{1in} and R_{1ex} obtained applying this fitting protocol are reported in Figure 5. The slight increase of R_{1ex} observed at ca. 1 MHz may be due to that, in the 2SX model, the compartment with lower R_1 is no longer the extracellular one as a consequence of the decrease of the intracellular relaxation rate. This can cause a slight error in the R_{1ex} estimation. The r_1 values obtained from the fitting (Figure 6), referred to the extracellular compartment, are reasonably similar to those one obtained for ProHance in Matrigel. This is the first time that an NMRD profile of a paramagnetic contrast agent is obtained in vivo after its distribution in the extracellular matrix of mammary tumour, taking into account the water exchange rate with the intracellular compartment. This finding gives further support to the view that the extracellular matrix in these type of tumours shows a slightly increased viscosity that, however, does not cause any dramatic change in the ProHance r_1. This could be due to the presence of a limited amount of proteins or other polymeric species (the "matrix") in these aggressive and partially necrotic tumours. In fact, the mobility of water appears similar to the one shown in a gel-like matrix as Matrigel that can be definitively considered a good model for the extracellular matrix in this kind of tumours. Finally, in the presence of clinical doses of Gd-CA, the magnetization recovery, in the investigated magnetic field strength range, can be well described by the 2SX model.

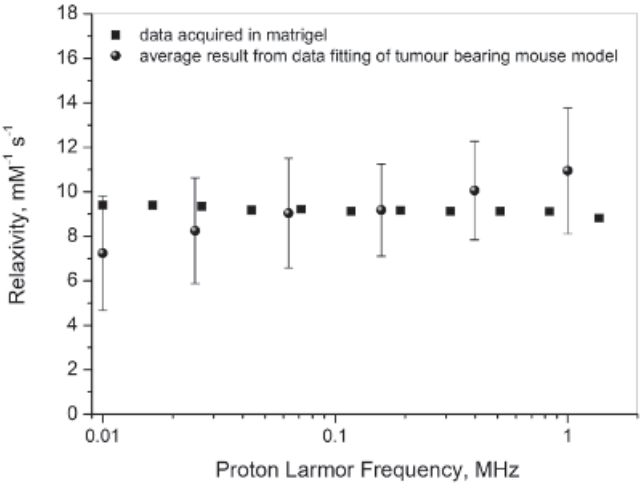

FIGURE 6 Relaxivity of ProHance dissolved in Matrigel (filled square) in comparison with the value obtained from the data fitting of tumour bearing mouse model (filled circle)

4 | CONCLUSION

Herein the first in vivo NMRD profiles for tumour tissues, obtained in the presence of a paramagnetic Gd-complex are reported. Upon the analysis of the experimental data obtained in the 0.01–1 MHz range by means of the 2SX procedure before the CA injection, it has been possible to extract the relaxation rate values for the extracellular and intracellular compartment ($R_{1ex}{}^0$ and R_{1in}), the intracellular water residence time (τ_{in}) and the intracellular water fraction ($V_{in} = 1\text{-}V_{ex}$). Fixing these values, it was then possible to extract the r_1 relaxivity of the paramagnetic agent in the extracellular compartment where it distributes. The obtained values are similar to those obtained when ProHance is dissolved in Matrigel that, therefore, results to be an excellent model to mimic the

characteristics of the extracellular compartment of the mammary tumours considered in this work.

The method, by assessing the relaxation properties of the extracellular space, will allow us to determine the effect of the "matrix" on the water proton relaxation times and, in turn, to get some insights of the composition of this compartment, till now, largely unknown. This open new horizon in the use of the fast field cycling MRI technologies that are currently under development for clinical use.[30,31]

ACKNOWLEDGEMENTS

This project has received funding from the European Union's Horizon 2020 framework programme under grant agreement number 668119 (project "IDentIFY"). This article is based upon work from COST (European Cooperation in Science and Technology) Action AC15209 (EURELAX).

ORCID

Simonetta Geninatti Crich https://orcid.org/0000-0003-2998-5424

REFERENCES

[1] L. M. Johnson, B. Turkbey, W. D. Figg, P. L. Choyke, *Nat. Rev. Clin. Oncol.* **2014**, *11*, 346.

[2] D. Leithner, G. J. Wengert, T. H. Helbich, S. Thakur, R. E. Ochoa-Albiztegur, E. A. Morris, K. Pinker, *Clin. Rad.* **2018**, *73*, 700.

[3] E. Rössler, C. Mattea, S. Stapf, *J. Magn. Reson.* **2015**, *251*, 43.

[4] K. J. Pine, G. R. Davies, D. J. Lurie, *J. Magn. Reson. Med.* **2010**, *63*, 1698.

[5] S. H. Koenig, R. D. Brown 3rd, D. Adams, D. Emerson, C. G. Harrison, *Invest. Radiol.* **1984**, *19*, 76.

[6] R. Kimmich, *Field-cycling NMR relaxometry: Instrumentation, model theories and applications*, RSC Publishing, Cambridge **2018**.

[7] S. H. Koenig, *Acad. Radiol.* **1996**, *3*, 597.

[8] M. R. Ruggiero, S. Baroni, S. Pezzana, G. Ferrante, S. Geninatti Crich, S. Aime, *Angew. Chem.* **2018**, *57*, 7468.

[9] C. S. Springer Jr., *J. Magn. Reson.* **2018**, *291*, 110.

[10] M. R. Ruggero, S. Baroni, S. Aime, S. Geninantti Crich, *Mol. Phys.* **2018**, 1. https://doi.org/10.1080/00268976.2018.1527045

[11] E. Gianolio, G. Ferrauto, E. Di Gregorio, S. Aime, *Biochim. Biophys. Acta Biomembr.* **2016**, *1858*, 627.

[12] C. S. Springer Jr., X. Li, L. A. Tudorica, K. Y. Oh, N. Roy, S. Y.-C. Chui, A. M. Naik, M. L. Holtorf, A. Afzal, W. D. Rooney, W. Huang, *NMR Biomed.* **2014**, *27*, 760.

[13] C. S. Landis, X. Lin, F. W. Telaqng, P. E. Molina, I. Palyka, G. Vetek, C. S. Springer Jr., *Magn. Reson. Med.* **1999**, *42*, 467.

[14] C. F. Hazlewood, D. C. Chang, B. L. Nichols, D. E. Woessner, *Biophys. J.* **1974**, *14*, 584.

[15] Y. Gossuin, C. Burtea, A. Monseux, G. Toubeau, A. Roch, R. N. Muller, P. Gillis, *J. Magn. Reson Imag.* **2004**, *20*, 690.

[16] S. H. Koenig, M. Spiller, R. D. Brown, G. L. Wolf, *Invest. Radiol.* **1986**, *21*, 697.

[17] M. Spiller, R. D. Brown, S. H. Koenig, G. L. Wolf, *Magn. Reson. Med.* **1988**, *8*, 293.

[18] C. S. Landis, X. Li, F. W. Telang, J. A. Coderre, P. L. Micca, W. D. Rooney, L. L. Latour, G. Vétek, I. Pályka, C. S. Springer Jr., *Magn. Reson. Med.* **2000**, *44*, 563.

[19] S. Aime, P. Caravan, *J. Magn. Reson. Imag.* **2009**, *30*, 1259.

[20] C. S. Hughes, L. M. Postovit, G. A. Lajoie, *Proteomics* **2010**, *10*, 1886.

[21] D. Delli Castelli, M. C. Caligara, M. Botta, E. Terreno, S. Aime, *Inorg. Chem.* **2013**, *52*, 7130.

[22] A. Fringuello Mingo, S. Colombo Serra, S. Baroni, C. Cabella, R. Napolitano, I. Hawala, I. M. Carnovale, L. Lattuada, F. Tedoldi, S. Aime, *Magn. Reson. Med.* **2017**, *78*, 1523.

[23] Y. Ayant, E. Belorizky, J. Alizon, J. Gallice, *J. Phys. (Paris)* **1975**, *36*, 991.

[24] L. P. Hwang, J. H. Freed, *J. Chem. Phys.* **1975**, *63*, 4017.

[25] D. Hugh Powell, O. M. Ni Dhubhghaill, D. Pubanz, L. Helm, Y. S. Lebedev, W. Schlaepfer, A. E. Merbach, *J. Am. Chem. Soc.* **1996**, *118*, 9333.

[26] É. Tóth, F. Connac, L. Helm, K. Adzamli, A. E. Merbach, *JBIC* **1998**, *3*, 606.

[27] S. L. Barnes, A. G. Sorace, M. E. Loveless, J. G. Whisenant, T. E. Yankeelov, *NMR Biomed.* **2015**, *28*, 1345.

[28] E. Panagiotaki, S. Walker-Samuel, B. Siow, S. P. Johnson, V. Rajkumar, R. B. Pedley, M. F. Lythgoe, D. C. Alexander, *Cancer Res.* **2014**, *74*, 1902.

[29] X. Li, W. D. Rooney, C. S. Springer Jr., *PNAS* **2008**, *105*, 17937.

[30] L. M. Broche, G. P. Ashcroft, D. J. Lurie, *Magn. Reson Med.* **2012**, *68*, 358.

[31] L. M. Broche, S. R. Ismail, N. A. Booth, D. J. Lurie, *Magn. Reson Med.* **2012**, *67*, 1453.

SUPPORTING INFORMATION

Additional supporting information may be found online in the Supporting Information section at the end of the article.

How to cite this article: Baroni S, Ruggiero MR, Aime S, Geninatti Crich S. Exploring the tumour extracellular matrix by in vivo Fast Field Cycling relaxometry after the administration of a Gadolinium-based MRI contrast agent. *Magn Reson Chem*. 2019;57:845–851. https://doi.org/10.1002/mrc.4837